



Title	Thermal properties of close-packed Fe up to 400 GPa determined using Hugoniot functions
Author(s)	Sano, Yukio; Sano, Tomokazu
Citation	Physical Review B. 2004, 69(14), p. 144201
Version Type	VoR
URL	https://hdl.handle.net/11094/89441
rights	Copyright 2004 by the American Physical Society
Note	

The University of Osaka Institutional Knowledge Archive : OUKA

<https://ir.library.osaka-u.ac.jp/>

The University of Osaka

Thermal properties of close-packed Fe up to 400 GPa determined using Hugoniot functions

Yukio Sano

Kobe University of Mercantile Marine (at present, Kobe University), Higashi-Nada-Ku, Kobe 658-0022, Japan

Tomokazu Sano*

Graduate School of Engineering, Osaka University, Suita, Osaka 565-0871, Japan

(Received 19 August 2003; revised manuscript received 23 January 2004; published 1 April 2004)

A quadratic equation for the temperature-independent Grüneisen coefficient γ was derived by a method in which the Walsh-Christian and Mie-Grüneisen equations are combined. Some previously existing *ab initio* temperature Hugoniots for hexagonal close-packed solid Fe are inaccurate because the constant-volume specific heats on the Hugoniots C_{VH} , which are related uniquely to the solutions of the quadratic equation, have values that are too small. A C_{VH} distribution in the solid phase range was demonstrated to agree approximately with a previous *ab initio* distribution. In contrast, the corresponding γ distribution was significantly different from the *ab initio* distribution in the lower pressure region, and the γ distribution in the liquid phase range had a considerably larger gradient than the *ab initio* distribution. The causes of these disagreements are clarified.

DOI: 10.1103/PhysRevB.69.144201

PACS number(s): 64.70.Dv, 64.30.+t, 62.50.+p, 47.40.Nm

I. INTRODUCTION

The thermoelastic properties of hexagonal close-packed (hcp) Fe at pressures up to 400 GPa were recently investigated using the *ab initio* approach. Wasserman, Stixrude, and Cohen¹ used a tight-binding total-energy method and the cell model of vibrational partition function, while the calculations of Alfè, Price, and Gillan² were based on density-function theory (DFT) using a generalized-gradient approximation. The Hugoniot pressures calculated by Cohen *et al.*¹ agreed almost perfectly with the experimental data of Brown and McQueen³ in the region of 150 to 240 GPa, as did the different statistical-mechanical calculations of Alfè *et al.*² The temperature Hugoniots calculated by Cohen *et al.* and Alfè *et al.* approximate those of Brown and McQueen.

The constant-volume specific heats on the isotherms calculated by Cohen *et al.*,¹ however, are significantly smaller than those of Alfè *et al.*² The main reason for this seems to be the anharmonic corrections included by Alfè *et al.*² Moreover, there is a crucial difference between the Grüneisen coefficients on isotherms in the lower pressure region in the solid phase range predicted by both groups. The distributions of Cohen *et al.* increase rapidly with a decrease in pressure in the lower pressure region, whereas those of Alfè *et al.* vary only slightly in the solid phase range. It is important that we clarify the cause of this enigmatic difference between these distributions in the lower pressure region, because assumptions or estimates of the values of the Grüneisen coefficient have a key role in constructing parametrized equations of the state for Fe.⁴ We attempted to investigate the cause of the difference by predicting the thermal properties of Fe using classical thermodynamics, and without relying on the *ab initio* method.

In this study, we derive a quadratic equation for the Grüneisen coefficient using a method that combines the Walsh-Christian equation^{5,6} and a Mie-Grüneisen equation integrated from a statically compressed state to a Hugoniot state at thermodynamic equilibrium. The assumptions used were that the constant-volume specific heat is a linear function of

temperature and that the Grüneisen coefficient is a function of specific volume alone. For solid Fe, the validity of these two assumptions was verified. We obtained the Hugoniot pressures included in the solution of the quadratic equation from the experimental Hugoniot for Fe of Brown *et al.*^{3,7} and the quasistatic pressures at an ambient temperature from the experimental equation of state for Fe of Mao *et al.*⁸ Unfortunately, there is no existing experimental temperature Hugoniot for Fe available from which the Hugoniot temperatures in the solution can be found. For the Hugoniot temperatures, therefore, we adopted the theoretical temperature Hugoniots for solid Fe of Cohen *et al.*,¹ Alfè *et al.*,² Brown and McQueen,³ and Alfè *et al.*⁴; for liquid Fe, we relied on the theoretical work of Alfè *et al.*⁴ and Belonoshko, Ahuja, and Johansson.⁹ Based on the experimental pressure Hugoniot and static equation of state, we assess the reliability of the above-mentioned temperature Hugoniots. The inaccuracy of some of the four temperature Hugoniots for solid Fe was found by showing that the constant-volume specific heats along the Hugoniots, which are related uniquely to the solutions of the quadratic equation, become smaller than their harmonic contribution. In addition, our Grüneisen coefficients for the temperature Hugoniots for solid and liquid Fe of Alfè *et al.*⁴ are compared with the *ab initio* result² and the result calculated by another thermodynamic formalism.¹⁰ Finally, we evaluate a thermal equation of state based on experimental data for hcp Fe by deducing the temperature Hugoniot, the constant-volume specific heat on the Hugoniot, and the Grüneisen coefficient from our alternate thermodynamic theory that incorporates the thermal equation of state.

II. THERMODYNAMIC THEORY**A. Quadratic equation for the Grüneisen coefficient**

The Walsh-Christian equation holds at the rear of a shock wave front:^{5,6}

$$C_{VH} \frac{dT_H}{dV_H} + \frac{\gamma_H}{V_H} C_{VH} T_H = F_H, \quad (1)$$

where

$$F_H = \frac{1}{2} \frac{dp_H}{dV_H} (V_0 - V_H) + \frac{1}{2} p_H, \quad (2)$$

where p is the pressure, T is the temperature, V is the specific volume, C_V is the constant-volume specific heat, and γ is the Grüneisen coefficient. The subscript 0 refers to an ambient state and the subscript H to a Hugoniot state, as in the example, $C_{VH} \equiv C_V(V_H, T_H) \equiv C_{VH}(V_H)$ and $\gamma_H \equiv \gamma(V_H, T_H) \equiv \gamma_H(V_H)$. The following Mie-Grüneisen equation is derived by integrating $dp = [\gamma(V, T)/V] C_V(V, T) dT$ along $V = \text{const}$ from a static compression state at an ambient temperature T_0 to a Hugoniot state:

$$p_H(V_H) - p_{T_0}(V) = \int_{T_0}^{T_H(V_H)} \frac{\gamma(V, T)}{V} C_V(V, T) dT, \quad (3)$$

where $V \equiv V_H$ and p_{T_0} is the quasistatic pressure at T_0 . Note that $C_V = C_{V\text{harm}} + C_{V\text{anharm}} + C_{V\text{el}}$, where the harmonic contribution to the constant-volume specific heat $C_{V\text{harm}}$ is equal to $3Nk_B$ to a good approximation (N being the number of atoms per unit mass and k_B is the Boltzmann constant), and where the anharmonic contribution $C_{V\text{anharm}}$ is proportional to T^2 . First, we assume that in the region of T_0 to T_H as defined in Eq. (3), the electronic contribution $C_{V\text{el}}$ is proportional to T . Then, because $C_{V\text{anharm}} + C_{V\text{el}} = \Gamma T$, where $\Gamma = \Gamma_{\text{anharm}} + \Gamma_{\text{el}}$, it follows that $C_V(V, T) = 3Nk_B + \Gamma(V)T$ in Eq. (3) and $C_{VH} = 3Nk_B + \Gamma(V_H)T_H$ in Eq. (1). Second, we assume that γ depends only on V , irrespective of T , in the region of T_0 to T_H . It then follows that $\gamma_H \equiv \gamma(V_H)$ in Eq. (1) and $\gamma(V, T) \equiv \gamma(V)$ in Eq. (3). For solid Fe, Secs. III A and III D verify the validity of the assumptions of linear $C_{V\text{el}}(T)$ and temperature independent γ , respectively. Equation (3) is integrated under the two assumptions described above to become

$$p_H - p_{T_0} = \frac{1}{2} \frac{\gamma}{V} (T_H - T_0) [6Nk_B + \Gamma(T_H + T_0)], \quad (4)$$

where $\Gamma \equiv \Gamma(V)$ and $\gamma \equiv \gamma(V)$. We assume that p_H , and hence dp_H/dV_H , and T_H , and hence dT_H/dV_H , are known. Two unknown variables C_{VH} or $\Gamma(V_H)$ and $\gamma(V_H)$ are then included in Eq. (1). If $p_{T_0}(V)$ is also assumed to be known, then in Eq. (4), $\Gamma(V)$ and $\gamma(V)$ appear as unknowns.

We transform Eq. (1) to the following equation for $\Gamma(V_H)$:

$$\Gamma = \frac{1}{T_H} \left[\frac{F_H}{dT_H/dV_H + (\gamma/V_H)T_H} - 3Nk_B \right]. \quad (5)$$

We also obtain an equation for $\Gamma(V_H)$, which is identical to $\Gamma(V)$, from Eq. (4):

$$\Gamma = \frac{2(p_H - p_{T_0})}{T_H^2 - T_0^2} \left(\frac{\gamma}{V_H} \right)^{-1} - \frac{6Nk_B}{T_H + T_0}, \quad (6)$$

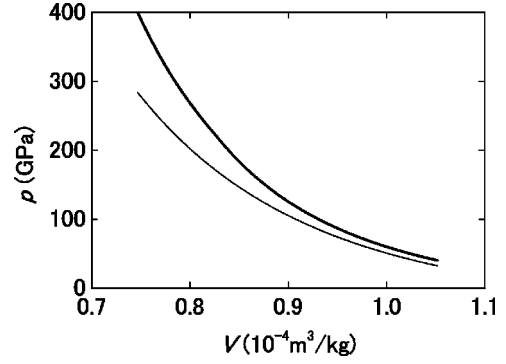


FIG. 1. $p_H(V_H)$ Hugoniot obtained using the quadratic $U_S - U_P$ relation of Brown *et al.* (Ref. 7) (heavy solid curve) and static pressure-volume distribution $p_{T_0}(V)$ of Mao *et al.* (Ref. 8) (solid curve).

where $p_{T_0} \equiv p_{T_0}(V)$, in which $V = V_H$, and $\gamma \equiv \gamma(V_H)$. We derive a quadratic equation for γ/V_H by equating Eqs. (5) and (6):

$$a \left(\frac{\gamma}{V_H} \right)^2 + b \left(\frac{\gamma}{V_H} \right) + c = 0, \quad (7)$$

where

$$\begin{aligned} a &= 3Nk_B(T_H - T_0)^2, \\ b &= \frac{T_H^2 - T_0^2}{T_H} F_H + 3Nk_B \frac{(T_H - T_0)^2}{T_H} \frac{dT_H}{dV_H} - 2(p_H - p_{T_0})T_H, \\ c &= -2(p_H - p_{T_0}) \frac{dT_H}{dV_H}, \end{aligned} \quad (8)$$

where $a > 0$, $b < 0$ because $F_H < 0$ and $dT_H/dV_H < 0$, and $c > 0$ for Fe in the pressure region of interest. For Fe, therefore, a nontrivial solution of Eq. (7) is given by

$$\frac{\gamma}{V_H} = \frac{-b - \sqrt{b^2 - 4ac}}{2a}. \quad (9)$$

Three quantities p_H , p_{T_0} , and T_H included in coefficients a , b , and c are obtained, respectively, from the experimental pressure Hugoniot of Brown *et al.*,^{3,7} the experimental equation of state of Mao *et al.*,⁸ and several *ab initio* temperature Hugoniot^{1,2,4,9} presented by many authors.

B. Experimental pressure Hugoniot and equation of state for Fe

Brown, Fritz, and Fixson⁷ refined the $U_S - U_P$ measurements for hcp Fe of Brown and McQueen³ and gave $U_S = 3.691 + 1.788U_P - 0.038U_P^2$ for a quadratic fit to the refined data, where U_S and U_P are in km/s. Brown¹¹ transformed the measured data into pressure-specific volume data up to 400 GPa using the Rankine-Hugoniot jump conditions (Fig. 1). Mao *et al.*⁸ reported the results of x-ray-diffraction experiments with the diamond anvil cell (DAC) to pressures above 300 GPa at room temperatures on hcp Fe and gave the

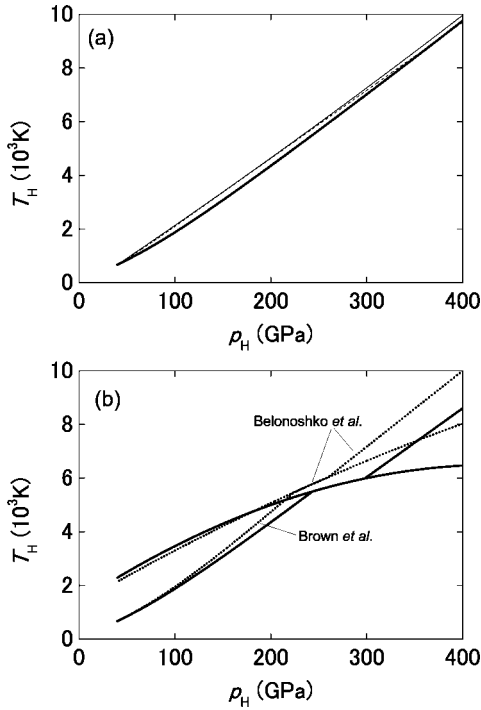


FIG. 2. (a) Solid Hugoniot of Cohen *et al.* (Ref. 1) (dashed curve), Alfè *et al.* (Ref. 2) (solid curve), and that calculated using Γ given by Eq. (10) (heavy solid curve). (b) Solid Hugoniot of Brown and McQueen, (Ref. 3) melting curve, and liquid Hugoniot of Belonoshko *et al.* (Ref. 9) (heavy dotted curves) and solid Hugoniot, melting curve, and liquid Hugoniot of Alfè *et al.* (Ref. 4) (heavy solid curves). All solid Hugoniot shown in (a) and (b) start from the point (40 GPa, 670 K). (Ref. 12).

Birch-Murnaghan equation of state parameters of $V_{02} = 6.73 \text{ cm}^3/\text{mol}$, $K_{02} = 165 \text{ GPa}$, and $K'_{02} = 5.33$. The Birch-Murnaghan equation of state $p_{T_0}(V)$ is shown in Fig. 1.

C. $T_H(p_H)$ solid Hugoniot for Fe

The *ab initio* $T_H(p_H)$ Hugoniot for hcp solid Fe of Cohen *et al.*¹ in the region from 40 to 400 GPa is approximated by a quadratic equation for $40 \leq p_H \leq 100$ GPa and by a linear equation for $100 < p_H \leq 400$ GPa. The $T_H(p_H)$ Hugoniot for $40 \leq p_H \leq 400$ GPa of Alfè *et al.*² also is approximated by a quadratic equation. The solid Hugoniot of both groups are shown in Fig. 2(a). From 40 to 200 GPa, the Hugoniot of Alfè *et al.*² is in good agreement with that of Cohen *et al.*¹

We can find a $T_H(p_H)$ solid Hugoniot which agrees well with the *ab initio* Hugoniot of Alfè *et al.*⁴ up to 243 GPa from Eq. (1) using the following linear $\Gamma(p_H)$ and the corresponding γ/V_H :

$$\Gamma(p_H) = a_\Gamma p_H + b_\Gamma, \quad (10)$$

where $a_\Gamma = -8.4904 \times 10^{-5} \text{ J/kg K}^2 \text{ GPa}$ and $b_\Gamma = 0.080145 \text{ J/kg K}^2$. The equation for γ/V_H , which is related to Γ , is obtained from Eq. (4):

$$\frac{\gamma}{V_H} = \frac{2(p_H - p_{T_0})}{(T_H - T_0)[6Nk_B + \Gamma(T_H + T_0)]}. \quad (11)$$

The $T_H(p_H)$ Hugoniot calculated using Eqs. (1), (10), and (11) under the initial condition of $T_H(p_H) = 670 \text{ K}$ at $p_H = 40 \text{ GPa}$ (Ref. 12) is shown in Fig. 2(a).

D. $T_H(p_H)$ solid Hugoniot, melting curves, and $T_H(p_H)$ liquid Hugoniot for Fe

Because the material in question is a mixture of a solid and a liquid on a melting curve [$T_m(p)$], all the results obtained for C_{VH} and γ are meaningless, even if T_m is used instead of T_H . Our calculations apply only to single-phase solids and liquids, but nevertheless the melting curve plays an important role in determining the melting incipience and completion states. Several independent attempts to obtain *ab initio* melting curves were recently reported.^{4,9} Belonoshko *et al.*⁹ presented a melting curve that is in agreement with DAC experimental melting data¹³ at low pressures and is in excellent agreement with the shock melting result of 5500 K at 243 GPa.³ Using Eqs. (1) and (11), and the equation $C_{VH} = 3Nk_B + \Gamma T_H[\Gamma = \beta_e(V_H/V_0)^{\gamma_e}]$ of Brown and McQueen,³ where $\beta_e = 0.0612 \text{ J/kg K}^2$ and $\gamma_e = 1.34$, we calculate a $T_H(p_H)$ solid Hugoniot that intersects the melting curve of Belonoshko *et al.*⁹ at 221 GPa; we approximate the *ab initio* $T_H(p_H)$ liquid Hugoniot of Belonoshko *et al.*⁹ by a linear equation in the region above 260 GPa. Our value of $\beta_e = 0.0612 \text{ J/kg K}^2$ is smaller than that of 0.091 J/kg K^2 used by Brown and McQueen,³ and our value of $\gamma_e = 1.34$ is the same as that used by Brown and McQueen.³ The solid Hugoniot, melting curve, and liquid Hugoniot are shown in Fig. 2(b).

Alfè *et al.*⁴ constructed an improved DFT, which corrected free energy F in their previous DFT;² in addition they presented a melting curve with an F correction, which is in quite good agreement with the measurement of Shen *et al.*¹⁴ and with the shock melting result of 5500 K at 243 GPa.³ Finally, Alfè *et al.*⁴ introduced a $T_H(p_H)$ solid Hugoniot up to 243 GPa and a $T_H(p_H)$ liquid Hugoniot from 298 GPa that corrected F for consistency. The solid Hugoniot with the F correction is very close to our solid Hugoniot that was calculated using Eq. (10) and illustrated in Fig. 2(a). Therefore, we use our Hugoniot up to 243 GPa, where it intersects the melting curve of Alfè *et al.*⁴ The liquid Hugoniot is approximated by a linear equation. The solid Hugoniot, melting curve, and liquid Hugoniot are shown in Fig. 2(b).

Laio *et al.*¹⁵ also calculated a melting curve for Fe using their *ab initio* method. Boehler and co-workers¹⁶ compared the melting curves of Belonoshko *et al.*,⁹ Laio *et al.*,¹⁵ and Alfè *et al.*¹⁷ with the DAC data of Boehler^{13,18} and demonstrated that only the results of Laio *et al.*,¹⁵ which are considerably lower than the others, are comparable with the DAC data. On the other hand, the experimental melting curve of Yoo *et al.*¹⁹ is considerably higher than those of Belonoshko *et al.*⁹ and Alfè *et al.*^{4,17} in the pressure region of interest. Burakovsky *et al.*²⁰ presented a theory of the melting of elements as a dislocation-mediated phase transition. Burakovsky *et al.*²¹ derived an equation for the pressure dependence of the melting temperatures of the elements, calculated the melting curves for 24 elements, and obtained good agreement with existing experimental data. For Fe, however,

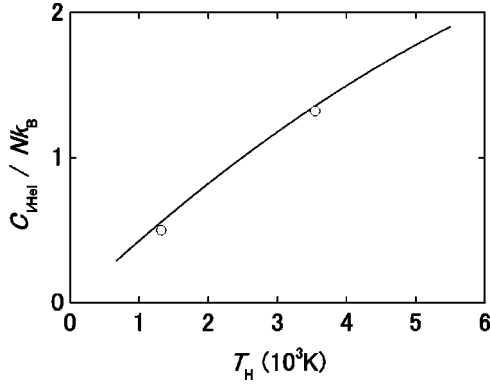


FIG. 3. Electronic specific heat $C_{V\text{Hel}}/Nk_B$ in the solid phase range calculated from $[\Gamma(p_H)T_H - ab\ initio\ C_{V\text{H}\text{an}\text{harm}}]/Nk_B$ using *ab initio* $C_{V\text{H}\text{an}\text{harm}}$ formulated by incorporating the specific-heat data of Alfè *et al.* (Ref. 2) (solid curve) and *ab initio* $C_{V\text{Hel}}/Nk_B$ of Alfè *et al.* (Ref. 2) at $T_H = 3546$ K for atomic volumes $8\ \text{\AA}^3$ and $T_H = 1318$ K for $9\ \text{\AA}^3$ (circles).

the curve is a little higher than that of Yoo *et al.*¹⁹ We chose the melting curves of Belonoshko *et al.*⁹ and Alfè *et al.*⁴ because they are in good agreement with the DAC data at low pressures and with the estimate based on the shock data at 243 GPa.

III. THERMAL PROPERTIES

A. Validity of linear $C_{V\text{el}}(T)$ assumption

Alfè *et al.*² calculated the electronic specific heat $C_{\text{perf}}(T)[\equiv C_{V\text{el}}]$ of the rigid perfect lattice for hcp solid Fe in the region of 0 to 6000 K using the *ab initio* method and plotted the resulting values for atomic volumes of $7.0\ \text{\AA}^3$ ($V_H = 0.7548 \times 10^{-4}\ \text{m}^3/\text{kg}$ and $p_H = 377.1$ GPa), $8.0\ \text{\AA}^3$ ($V_H = 0.8627 \times 10^{-4}\ \text{m}^3/\text{kg}$, $p_H = 166.8$ GPa, and $T_H = 3546$ K), $9.0\ \text{\AA}^3$ ($V_H = 0.9705 \times 10^{-4}\ \text{m}^3/\text{kg}$, $p_H = 73.75$ GPa, and $T_H = 1318$ K), and $10.0\ \text{\AA}^3$. In these equations, p_H was calculated from V_H using the $P_H(V_H)$ Hugoniot of Brown *et al.*^{3,7} and T_H was then calculated from p_H using the $T_H(p_H)$ solid Hugoniot of Alfè *et al.*⁴ The $C_{\text{perf}}(T)$ distribution for $7\ \text{\AA}^3$ is the closest to a straight line. When the volume is large, the deviation of the distribution from a straight line is also large in the whole region of 0 to 6000 K, but it does not become large in a portion of T_0 to T_H , defined in Eq. (3), because T_H is lower than 6000 K. The deviations over the region of T_0 to T_H for the volumes of interest are not great, so we consider that our assumption regarding the constant-volume heat in the region of T_0 to T_H , expressed by $C_{V\text{el}} = \Gamma_{\text{el}}T$ or $C_V = 3Nk_B + \Gamma T$, is valid.

To substantiate the validity of $C_{V\text{el}} = \Gamma_{\text{el}}T$ for hcp solid Fe, we evaluate $[\Gamma(p_H)T_H - ab\ initio\ C_{V\text{H}\text{an}\text{harm}}]$, where $\Gamma(p_H)$ is given by Eq. (10), and the *ab initio* $C_{V\text{el}}$ of Alfè *et al.*² We obtained *ab initio* $C_{V\text{H}\text{an}\text{harm}} = (1/6000)[0.28 + 0.25(V_A - V_H)/(V_A - V_B)]T_H Nk_B$, where $V_A = 7$ and $V_B = 10\ \text{\AA}^3$, using the *ab initio* specific-heat data of Alfè *et al.*² The calculated $[\Gamma(p_H)T_H - ab\ initio\ C_{V\text{H}\text{an}\text{harm}}]/Nk_B$ distribution as a function of the Hugoniot temperature T_H is shown in Fig. 3. The calculated distribution (solid curve)

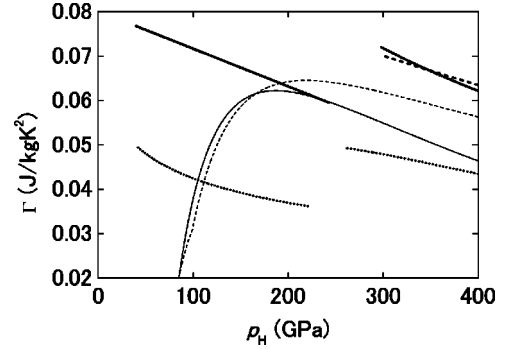


FIG. 4. Distributions of Γ for the solid Hugoniots of Cohen *et al.* (Ref. 1) (dashed curve), Alfè *et al.* (Ref. 2) (solid curve), Brown and McQueen (Ref. 3) (heavy dotted curve), and Γ given by Eq. (10) (heavy solid curve) as a function of Hugoniot pressure p_H . Γ distributions for the liquid Hugoniots from 260 to 400 GPa of Belonoshko *et al.* (Ref. 9) (heavy dotted curve), from 298 to 400 GPa of Alfè *et al.* (Ref. 4) (heavy solid curve), and from 298 to 400 GPa of Alfè *et al.* (Ref. 4) obtained by substituting $\gamma = 1.51$ into Eq. (5) (heavy dashed curve) are also shown.

is close to the values (circles) of the *ab initio* $C_{V\text{el}}$ of Alfè *et al.*² at $T_H = 3546$ K for $8\ \text{\AA}^3$ and $T_H = 1318$ K for $9\ \text{\AA}^3$, indicating that $[\Gamma(p_H)T_H - ab\ initio\ C_{V\text{H}\text{an}\text{harm}}] \approx ab\ initio\ C_{V\text{el}}$. This approximate equation can be transformed to *ab initio* $C_{V\text{el}} \approx [\Gamma(p_H) - ab\ initio\ \Gamma_{\text{an}\text{harm}}(V_H)]T_H$, that is, to *ab initio* $C_{V\text{el}} \approx \Gamma_{\text{el}}(V_H)T_H$. This means that the electronic specific heats at temperatures T within the regions of 0 to T_H for the specific volumes of interest V , $C_{V\text{el}}(V, T)$, are expressed approximately by $\Gamma_{\text{el}}(V)T$. The validity of our linear $C_{V\text{el}}(T)$ assumption was thus verified.

B. Constant-volume specific heat

The distributions of $\Gamma(p_H)$ for the $T_H(p_H)$ solid Hugoniots of Cohen *et al.*¹ and Alfè *et al.*² are obtained by substituting solution (9) into Eq. (6) [Fig. 4]. The difference between the two Γ distributions is due only to the difference between the $T_H(p_H)$ Hugoniots. Since the $T_H(p_H)$ Hugoniots of Cohen *et al.*¹ and Alfè *et al.*² are similar below 200 GPa, the $\Gamma(p_H)$ for both Hugoniots are also similar. Here we define the rejection of a set of T_H , C_{VH} , and γ (or γ_H) by the relationship $d\Gamma(p_H)/dp_H \geq 0$, because $d\Gamma_{\text{el}}/dp_H < 0^3$ and, as is clear from the *ab initio* $C_{V\text{H}\text{an}\text{harm}}$ derived above, $d\Gamma_{\text{an}\text{harm}}/dp_H < 0$. A situation in which $d\Gamma(p_H)/dp_H > 0$ might cause the values of C_{VH} to drop below $3Nk_B$, that is, below the harmonic contribution value. The $T_H(p_H)$ Hugoniots of Cohen *et al.*¹ and Alfè *et al.*² are not correct in the regions below at least 210 and 180 GPa, respectively. The $p_H(V_H)$ Hugoniots of both groups^{1,2} greatly deviate from the experimental Hugoniot used in our calculations in the pressure region below 150 GPa; thus, this deviation may result in regions where $d\Gamma(p_H)/dp_H \geq 0$.

The distributions of $\Gamma(p_H)$ for the $T_H(p_H)$ liquid Hugoniots of Alfè *et al.*⁴ and Belonoshko *et al.*⁹ are shown in Fig. 4. The $\Gamma(p_H)$ distribution for the $T_H(p_H)$ liquid Hugoniot of Alfè *et al.*⁴ is almost parallel to and is greatly above the

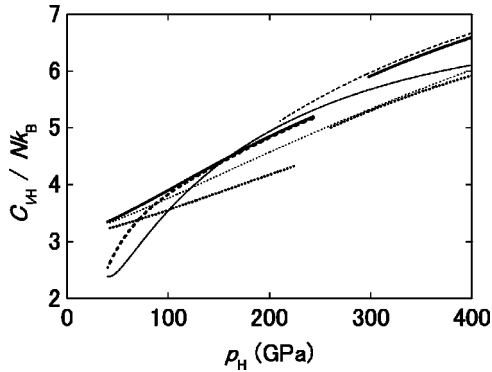


FIG. 5. Distributions of constant-volume specific heat C_{VH}/Nk_B obtained using Γ for the solid Hugoniot of Cohen *et al.* (Ref. 1) (dashed curve), Alfè *et al.* (Ref. 2) (solid curve), Brown and McQueen (Ref. 3) with $\beta_e=0.0612$ (heavy dotted curve) and 0.091 J/kg K^2 (dotted curve), Γ given by Eq. (10) (heavy solid curve), and Γ for the solid Hugoniot of Alfè *et al.* (Ref. 4) obtained using estimated γ_H (heavy dashed curve) as a function of Hugoniot pressure p_H . Distributions of C_{VH} obtained using Γ for the liquid Hugoniot from 260 to 400 GPa of Belonoshko *et al.* (Ref. 9) (heavy dotted curve) and from 298 to 400 GPa of Alfè *et al.* (Ref. 4) (heavy solid curve) are also shown.

linear $\Gamma(p_H)$ distribution (Fig. 4) in the solid phase range given by Eq. (10). The same is true for the $\Gamma(p_H)$ distribution for the $T_H(p_H)$ liquid Hugoniot of Belonoshko *et al.*,⁹ although the $\Gamma(p_H)$ distribution (Fig. 4) of Brown and McQueen³ with $\beta_e=0.0612 \text{ J/kg K}^2$ and $\gamma^e=1.34$ is not linear.

The $C_{VH}(p_H)/Nk_B$ distributions calculated using the $\Gamma(p_H)$ distributions described above are shown in Fig. 5. A portion of the small $C_{VH}(p_H)$ on the $T_H(p_H)$ Hugoniot of Cohen *et al.*¹ below 210 GPa was excluded, and the distribution of Brown and McQueen³ with $\beta_e=0.091 \text{ J/kg K}^2$ and $\gamma^e=1.34$ was added. The $C_{VH}(p_H)/Nk_B$ on the $T_H(p_H)$ Hugoniot of Alfè *et al.*² decreases greatly with a decrease in p_H from about 180 GPa, reaches a value of 3 at about 70 GPa, and further lowers until p_H reaches 40 GPa. Thus, the C_{VH} distribution includes a region of disagreement from 70 to 180 GPa where $d\Gamma/dp_H \geq 0$ and $C_{VH} \geq 3Nk_B$ and an unphysical portion from 40 to 70 GPa where $d\Gamma/dp_H \geq 0$ and $C_{VH} < 3Nk_B$. The $C_{VH}(p_H)$ distribution of Brown and McQueen³ with $\beta_e=0.091 \text{ J/kg K}^2$ and $\gamma^e=1.34$ is acceptable because $d\Gamma(p_H)/dp_H < 0$, but it is lower than that on the $T_H(p_H)$ Hugoniot of Alfè *et al.*⁴ This difference can be explained by the anharmonic contribution neglected by Brown and McQueen.³ In fact, in the solid phase range, $[\beta_e(V_H/V_0)^{\gamma^e} T_H + ab\text{ initio } C_{VH\text{anharmonic}}]$ coincides almost perfectly with $\Gamma(p_H)T_H$, where $\Gamma(p_H)$ [$d\Gamma(p_H)/dp_H < 0$] is given by Eq. (10). In the liquid phase range, the $T_H(p_H)$ Hugoniot of Belonoshko *et al.*⁹ and Brown and McQueen³ with $\beta_e=0.091 \text{ J/kg K}^2$ and $\gamma^e=1.34$ are close and both $C_{VH}(p_H)$ distributions are also similar, as shown in Fig. 5.

Here we compare the constant-volume specific heat on the $T_H(p_H)$ solid Hugoniot of Alfè *et al.*,⁴ $C_{VH} [= 3Nk_B + \Gamma(p_H)T_H]$, with the *ab initio* C_{VH} of Alfè *et al.*² By substituting *ab initio* $C_{VH\text{el}} \approx \Gamma(p_H)T_H$

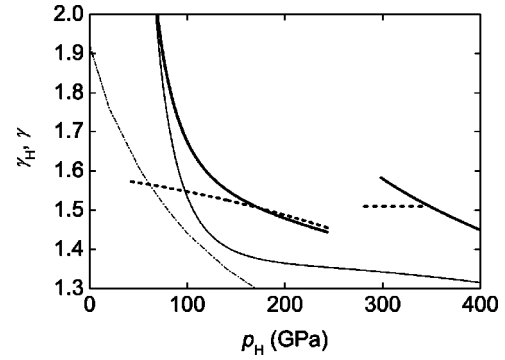


FIG. 6. Distributions of the Grüneisen coefficient γ for the solid Hugoniot of Alfè *et al.* (Ref. 2) (solid curve), γ for the solid and liquid Hugoniot of Alfè *et al.* (Ref. 4) (heavy solid curve), *ab initio* γ_H estimated from the *ab initio* γ_{isoth} distributions on isotherms in the solid phase range and *ab initio* γ_H in the liquid phase range of Alfè *et al.* (Ref. 2) (heavy dashed curve) as a function of Hugoniot pressure p_H , and $\gamma(p)$ along the melting curve of Anderson and Isaak (Ref. 10) (chain curve).

– *ab initio* $C_{VH\text{anharmonic}}$ revealed above into *ab initio* $C_{VH} = 3Nk_B + ab\text{ initio } C_{VH\text{anharmonic}} + ab\text{ initio } C_{VH\text{el}}$, we obtain *ab initio* $C_{VH} \approx 3Nk_B + \Gamma(p_H)T_H$. Therefore, $C_{VH} \approx ab\text{ initio } C_{VH}$.

C. Temperature-independent Grüneisen coefficient

The distributions of $\gamma(p_H)$ for the $T_H(p_H)$ solid Hugoniot of Alfè *et al.*² and Alfè *et al.*⁴ calculated using Eq. (9) and Eq. (11), respectively, are shown in Fig. 6. As was the case with the γ distribution of Cohen *et al.*,¹ both γ distributions increase rapidly with a decrease in p_H . An *ab initio* $\gamma_H(p_H)$ distribution is estimated from the *ab initio* $\gamma_{\text{isoth}}(p)$ distributions of Alfè *et al.*² on isotherms at 2000 and 4000 K in the solid phase range below 243 GPa (heavy dashed curve in Fig. 6). In the region of 170 to 243 GPa, the estimated γ_H distribution is just above the γ distribution for the $T_H(p_H)$ solid Hugoniot of Alfè *et al.*⁴ As p_H decreases from about 170 GPa, γ increases rapidly up to 3.8 at 40 GPa, but γ_H increases only a little. We find that while $C_{VH} \approx ab\text{ initio } C_{VH}$ in the solid phase range as demonstrated above, the difference between both distributions is significantly large in this lower pressure region. Because the *ab initio* $p_H(V_H)$ Hugoniot of Alfè *et al.*⁴ agrees well with the experimental data^{3,7} in the region above about 80 GPa, the experimental Hugoniot used in our calculations could not have caused the difference from the γ_H distribution above 80 GPa. This suggests that the *ab initio* method may be incomplete in some manner that is responsible for the prediction of the significantly lower distribution of the Grüneisen coefficient in the lower pressure region.

We can use our method to investigate the cause of the significantly lower γ_H distribution by predicting the C_{VH} corresponding to the estimated *ab initio* γ_H . Note that when γ_H is given, there is a C_{VH} that provides the same Hugoniot temperature as the T_H of Alfè *et al.*⁴ We substitute the *ab initio* γ_H into $\gamma (\equiv \gamma_H)$ in Eq. (5) and obtain the C_{VH} distribution on the $T_H(p_H)$ solid Hugoniot of Alfè *et al.*⁴ by

evaluating Eq. (5) (heavy dashed curve in Fig. 5). The Hugoniot C_{VH} distribution comprises three regions: an acceptable region above about 140 GPa where $d\Gamma/dp_H < 0$, which is close to the C_{VH} distribution obtained from the linear Γ given by Eq. (10); an unacceptable portion from about 55 to 140 GPa where $d\Gamma/dp_H \geq 0$ and $C_{VH} \geq 3Nk_B$, in which this function is lower than the C_{VH} distribution obtained from the linear Γ ; and an unphysical portion below 55 GPa where $d\Gamma/dp_H \geq 0$ and $C_{VH} < 3Nk_B$. The unacceptable and unphysical portions of C_{VH} thus result from the significantly lower γ_H distribution in the region below 140 GPa. In contrast, in the *ab initio* method² mentioned above, the acceptable C_{VH} near the constant-volume specific heat obtained from the linear Γ corresponds to the significantly smaller γ_H . This indicates that the *ab initio* method incorrectly predicted the Grüneisen coefficient. The *ab initio* method^{2,4} should be improved so that a set of T_H , C_{VH} , and γ_H would be correctly deduced.

A distribution of $\gamma(p_H)$ for the $T_H(p_H)$ liquid Hugoniot of Alfè *et al.*,⁴ calculated using Eq. (9), is shown in Fig. 6. γ is larger at the melting completion pressure of 298 than at the melting incipience pressure of 243 GPa. Equation (11) indicates that this is due to the larger value of $(p_H - p_{T_0})$ at 298 GPa, in spite of the smaller value of V_H and the larger values of T_H and Γ (Fig. 4) at 298 GPa. Note that the value of γ at 298 GPa varies with the gradient of the liquid Hugoniot, because Γ depends on dT_H/dV_H [see Eq. (5)]. On the other hand, γ also decreases with an increase in p_H in the liquid phase range, as was the case in the solid phase range. This is due to the decrease in V_H and the increase in T_H in spite of the decrease in Γ with increasing p_H .

The *ab initio* $\gamma_H(p_H)$ distribution of Alfè *et al.*² in the liquid phase range from 280 to 340 GPa (heavy dashed curve, $\gamma_H \approx 1.51$) is shown in Fig. 6. The *ab initio* γ_H distribution approximates the γ distribution (heavy solid curve) for the liquid Hugoniot of Alfè *et al.*⁴ although the difference in slope between both distributions is large. To investigate the cause of the large slope difference, we evaluate Γ for the liquid Hugoniot of Alfè *et al.*⁴ by substituting $\gamma_H = 1.51$ into Eq. (5). The Γ distribution evaluated from 298 to 400 GPa (heavy dashed curve) is shown in Fig. 4. Both Γ distributions (heavy dashed and solid curves) have a slope difference. Thus, the slope difference between both of the Γ (or C_{VH}) distributions caused the large slope difference between the γ_H and γ distributions.

Anderson and Isaak¹⁰ found the Grüneisen parameter $\gamma(p)$ along the melting curve $T_m(p)$ of hcp Fe by a method of combining the Lindemann melting equation with the Vinet equation of state at T_{m_0} , where T_{m_0} is the melting temperature at $p=0$. They assumed $\gamma(V) = \gamma_0(V/V_0)^q$, where q is a constant and V_0 is the specific volume at the initial state of $p=0$ and $T_m = T_{m_0}$, and transformed $\gamma(V) = \gamma_0(V/V_0)^q$ to the $\gamma(p)$ for $q=1$, $\gamma_0=1.92$, and $T_{m_0}=1600$ K by further assuming $C_V = 3Nk_B$ (chain curve in Fig. 6). In the solid phase range, their $\gamma(p)$ distribution also increases rapidly with a decrease in p , but the overall magnitude is consider-

ably lower than the distributions for the $T_H(p_H)$ solid and liquid Hugoniots of Alfè *et al.*⁴

D. Temperature dependence of the Grüneisen coefficient

We derived Eq. (9) from Eqs. (1) and (3) under the assumption that the Grüneisen coefficient is temperature independent. However, the *ab initio* coefficients γ_{isoth} on isotherms at 2000, 4000, and 6000 K of Cohen *et al.*¹ and Alfè *et al.*² showed that the Grüneisen coefficient is temperature dependent. Although the temperature dependent $\gamma(V_H, T_H)$ cannot be determined uniquely from Eqs. (1) and (3) alone, we deduce γ_H in the solid phase range from Eq. (1) using Eq. (10) and the Hugoniot shifted from the $T_H(p_H)$ solid Hugoniot of Alfè *et al.*⁴ Using the deduced γ_H , we then attempt to obtain γ_{isoth} from $\gamma(V, T) = \gamma_i(V) + w(V)T$ expressed by the sum of a temperature-independent term, $\gamma_i(V)$, and a temperature-dependent term, $w(V)T$. It follows that $\gamma_H = \gamma_i(V_H) + w(V_H)T_H$ on a Hugoniot. We derive the following equation for $w(p_H)$ by substituting $\gamma(V, T)$ into Eq. (3):

$$w = \frac{V_H(p_H - p_{T_0}) - \gamma_H d}{e - T_H d}, \quad (12)$$

where

$$d = 3Nk_B(T_H - T_0) + \frac{1}{2}\Gamma(T_H^2 - T_0^2),$$

$$e = \frac{3}{2}Nk_B(T_H^2 - T_0^2) + \frac{1}{3}\Gamma(T_H^3 - T_0^3), \quad (13)$$

where $\Gamma(p_H)$ is given by Eq. (10). We first deduce $w(p_H)$ from Eq. (12) using the shifted $T_H(p_H)$ Hugoniot, then obtain $\gamma_i(p_H)$ from $\gamma_i = \gamma_H - wT_H$, and finally determine $\gamma_{\text{isoth}}(p)$. Here, $\gamma_{\text{isoth}}(p) = \gamma_i(p) + w(p)T_{\text{isoth}}$, where $\gamma_i(p) \equiv \gamma_i(p_H)$ and $w(p) \equiv w(p_H)$.

We now verify the validity of our assumption concerning the Grüneisen coefficient. We evaluate $w(p_H)$ in the case in which the shifted Hugoniot is lower than the $T_H(p_H)$ solid Hugoniot of Alfè *et al.*⁴ by 12 K at 243 GPa (for the sake of simplicity, only the maximum difference between both Hugoniots is noted). In this case, w was clearly negative between 175 and 243 GPa. We find that $w < 0$ appeared in the *ab initio* result² of Cohen *et al.*¹ Figure 7(a) illustrates our γ_{isoth} distributions on isotherms at 2000 and 4000 K in the case where the shifted Hugoniot is higher by 12 K at 243 GPa, together with the *ab initio* results of Alfè *et al.*² Here, the shift of the solid Hugoniot was adjusted so that the following three conditions would be satisfied: (1) Our γ_{isoth} distribution on an isotherm at 2000 K is close to that of Alfè *et al.*² at 243 GPa; (2) the same is true for the γ_{isoth} distribution on the isotherm at 4000 K; and (3) $w > 0$ and the forms of both γ_{isoth} distributions on the isotherm at 2000 K (and 4000 K) do not differ greatly in the pressure region of interest. We find that w is clearly positive between 130 and 243 GPa and that our γ_{isoth} distributions on the isotherms at 2000 K and 4000 K approximately satisfy the three conditions [Fig. 7(a)]. Our γ_{isoth} distribution on the isotherm at 2000 K is close to that of Alfè *et al.*² from about 140 to 243 GPa, but both distributions rapidly part with a decrease in pressure

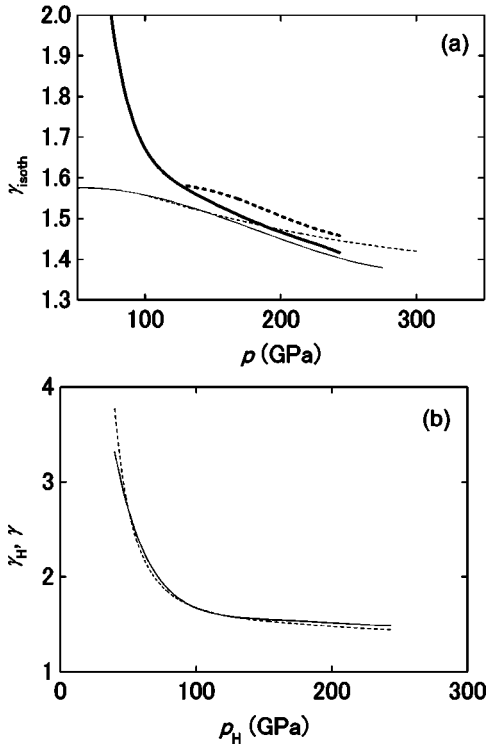


FIG. 7. (a) Distributions of the Grüneisen coefficient γ_{isoth} on isotherms at 2000 (heavy solid curve) and 4000 K (heavy dashed curve) and *ab initio* γ_{isoth} on isotherms at 2000 (solid curve) and 4000 K (dashed curve) of Alfè *et al.* (Ref. 2) as a function of pressure p . (b) Distributions of temperature-dependent Grüneisen coefficient γ_H in the solid phase range (solid curve) and temperature-independent γ for the solid Hugoniot of Alfè *et al.* (Ref. 4) (dashed curve) as a function of Hugoniot pressure p_H .

from 140 GPa. A calculated γ_H distribution and the γ distribution depicted in Fig. 6 are shown in Fig. 7(b). The difference between these distributions is slight. Thus, the Grüneisen coefficient is only slightly temperature dependent.²²

E. Sound velocity

We calculate adiabatic sound velocities in the liquid phase range above 298 GPa using the equation $C_s = (V_H/V_0)U_S[1 + s\epsilon_H - sV_0(\gamma/V_H)\epsilon_H^2]/(1 - s\epsilon_H)$,³ where $c = 4089.0$ m/s, $s = 1.5470$, $\epsilon_H = U_P/U_S$, and γ is the Grüneisen coefficient for the $T_H(p_H)$ liquid Hugoniot of Alfè *et al.*⁴ The values of c and s were obtained by fitting $U_S = c + sU_P$ to the refined $U_S - U_P$ data of Brown *et al.*⁷ in the region above 260 GPa. In Fig. 8, our calculated C_s distribution is compared with the experimental sound velocity data in the liquid phase range above 260 GPa of Brown and McQueen³ and Nguyen and Holmes.²³ Our sound velocity curve agrees well with the experimental data.

IV. THERMAL EQUATION OF STATE

Dubrovinsky *et al.*²⁴ collected the experimental data of Mao *et al.* (300 K),⁸ Jephcoat *et al.* (300 K),²⁵ Huang *et al.* (723 K),²⁶ Funamori *et al.* (950–1050, 1150–1250 K),²⁷ and Saxena *et al.* (300, 650–750, 950–1050, 1150–1250

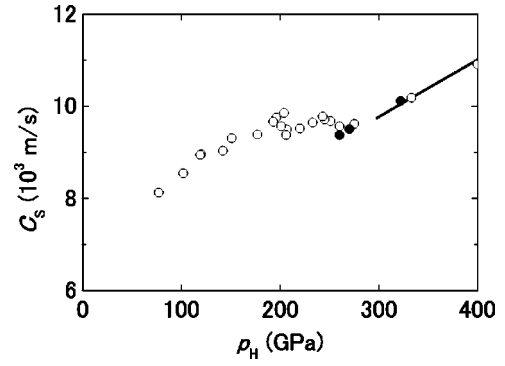


FIG. 8. Sound velocity distribution for the liquid Hugoniot from 298 to 400 GPa of Alfè *et al.* (Ref. 4) (heavy solid curve) as a function of Hugoniot pressure p_H and the experimental data for sound velocity of Brown and McQueen (Ref. 3) (circles) and Nguyen and Holmes (Ref. 23) (solid circles).

K),^{24,28–31} and determined a thermal equation of state of hcp Fe. We can obtain a static pressure at a temperature T_1 higher than T_0 , $p_{T_1}(V)$, from their thermal equation of state. Further using a Mie-Grüneisen equation including T_1 and $p_{T_1}(V)$, we here construct a thermodynamic theory from which T_H , C_{VH} , and γ can be deduced.

Under the same assumptions as those used in Sec. II A, that is, $C_V(V, T) = 3Nk_B + \Gamma(V)T$ and $\gamma(V, T) \equiv \gamma(V)$, the following Mie-Grüneisen equation, integrated from a static compression state at T_1 to a Hugoniot state, is derived:

$$p_H - p_{T_1} = \frac{1}{2} \frac{\gamma}{V} (T_H - T_1) [6Nk_B + \Gamma(T_H + T_1)], \quad (14)$$

where p_{T_1} is obtained from the thermal equation of state of Dubrovinsky *et al.*²⁴ Equations (4) and (14), in which $V \equiv V_H$, yield an equation for $\Gamma(p_H)$ including an unknown variable T_H :

$$\Gamma = \frac{6Nk_B[(T_H - T_1)(p_H - p_{T_0}) - (T_H - T_0)(p_H - p_{T_1})]}{(T_H^2 - T_0^2)(p_H - p_{T_1}) - (T_H^2 - T_1^2)(p_H - p_{T_0})}. \quad (15)$$

TABLE I. Hugoniot temperatures T_H , constant-volume specific heats on the Hugoniot C_{VH}/Nk_B , and Grüneisen coefficients γ for some solid Hugoniot pressures p_H calculated for $T_1 = 500$ K.

p_H (GPa)	T_H (K)	C_{VH}/Nk_B	γ
40	6.11	3.00	3.65
60	219	2.79	3.85
80	237	2.75	4.01
100	243	2.72	4.15
120	246	2.70	4.26
140	247	2.68	4.36
160	247	2.66	4.44
180	193	2.72	4.52
200	212	2.68	4.59
220	3290	-2.11	4.65
243	4710	-4.63	4.71

When Eq. (11) for γ/V_H and Eq. (15) are incorporated in Eq. (1), Eq. (1) has only T_H as unknown. We first calculate T_H using Eq. (1), then $\Gamma(p_H)$ from Eq. (15) using the T_H , and finally $\gamma(p_H)$ from Eq. (11) using the T_H and $\Gamma(p_H)$.

We calculated T_H , C_{VH} , and γ in the solid phase range from 40 to 243 GPa for T_1 between 300 and 1250 K using the thermoelastic parameters determined by Dubrovinsky *et al.*²⁴ However, as shown in Table I for $T_1=500$ K as an example, we could not obtain meaningful results for the three variables for any T_1 , suggesting that their thermal equation of state is not sufficiently precise to determine these variables. The necessity of a more precise thermal equation of state might be suggested by Eq. (15). The first term in the bracket of the numerator of the right side of Eq. (15), $(T_H - T_1)(p_H - p_{T_0})$, has a value near that of the second term, $(T_H - T_0)(p_H - p_{T_1})$. The same is true for the denominator.

V. CONCLUSIONS

The Grüneisen coefficients γ and the constant-volume specific heats C_{VH} on Hugoniot for solid and liquid Fe were evaluated using thermodynamic relations derived by a method that combines the Walsh-Christian and Mie-

Grüneisen equations. The validity of our assumptions that γ is a function of specific volume alone and that C_V is a linear function of temperature was verified in the solid phase range. We tested the reliability of the *ab initio* results using the thermodynamic relations including reliable experimental data. We found that two previously existing *ab initio* temperature Hugoniot are inaccurate and that the *ab initio* method incorrectly predicted a γ_H distribution which is significantly lower than our γ distribution in the lower pressure region in the solid phase range. The reliability of the *ab initio* results should be also assessed using these thermodynamic relations in the *ab initio* calculations, and any needed improvements implemented. In the liquid phase range, the *ab initio* γ_H distribution had a smaller gradient than our γ distribution. This difference was caused by a smaller slope of the Γ distribution corresponding to the γ_H distribution. The sound velocities calculated using this γ distribution agreed well with the experimental data.

ACKNOWLEDGMENT

The authors wish to thank Dr. Alfè of University College London for helpful discussions.

*Electronic address: sano@mapse.eng.osaka-u.ac.jp.

¹E. Wasserman, L. Stixrude, and R.E. Cohen, Phys. Rev. B **53**, 8296 (1996).

²D. Alfè, G. Price, and M. Gillan, Phys. Rev. B **64**, 045123 (2001).

³J. Brown and R. McQueen, J. Geophys. Res. **91**, 7485 (1986).

⁴D. Alfè, G. Price, and M. Gillan, Phys. Rev. B **65**, 165118 (2002).

⁵J. Walsh and R. Christian, Phys. Rev. **97**, 1544 (1955).

⁶T. Sano and Y. Sano, J. Appl. Phys. **90**, 3754 (2001).

⁷J. Brown, J. Fritz, and R. Hixson, J. Appl. Phys. **88**, 5496 (2000).

⁸H. Mao, Y. Wu, L. Chen, J. Shu, and A. Jephcoat, J. Geophys. Res. **95**, 21737 (1990).

⁹A. Belonoshko, R. Ahuja, and B. Johansson, Phys. Rev. Lett. **84**, 3638 (2000).

¹⁰O. Anderson and D. Isaak, Am. Mineral. **85**, 376 (2000).

¹¹J. Brown, Geophys. Res. Lett. **28**, 4339 (2001).

¹²J. Boettger and D. Wallace, Phys. Rev. B **55**, 2840 (1997).

¹³R. Boehler, Geophys. Res. Lett. **13**, 1153 (1986).

¹⁴G. Shen, H. Mao, R. Hemley, T. Duffy, and M. Rivers, Geophys. Res. Lett. **25**, 373 (1998).

¹⁵A. Laio, S. Bernard, G. Chiarotti, S. Scandolo, and E. Tosatti, Science **287**, 1027 (2000).

¹⁶D. Erradonea, B. Schwager, R. Ditz, C. Gessmann, R. Boehler, and M. Ross, Phys. Rev. B **63**, 132104 (2001).

¹⁷D. Alfè, M. Gillan, and G. Price, Nature (London) **401**, 462 (1999).

¹⁸R. Boehler, Rev. Geophys. **38**, 221 (2000).

¹⁹C. Yoo, N. Holmes, M. Ross, D. Webb, and C. Pike, Phys. Rev. Lett. **70**, 3931 (1993).

²⁰L. Burakovsky, D. Preston, and R. Silbar, Phys. Rev. B **61**, 15 011 (2000).

²¹L. Burakovsky, D. Preston, and R. Silbar, J. Appl. Phys. **88**, 6294 (2000).

²²The reasons why we adopted $w(V)T$ into the temperature-dependent part are as follows: The Grüneisen coefficient at zero pressure and temperature T can be shown to be a linear function of temperature in the region below 2000 K to a good approximation by calculating a thermodynamic relationship $\gamma_{T,0} = (\alpha_{T,0} K_{T,0} V_{T,0}) / (C_V)_{T,0}$ using the constant-volume specific heat $(C_V)_{T,0} = 3Nk_B + \Gamma_1 T$, the bulk modulus $K_{T,0} = (b_0 + b_1 T + b_2 T^2)^{-1}$, the thermal expansivity $\alpha_{T,0} = a_0 + a_1 T + a_2 T^{-2}$, and the specific volume $V_{T,0} = V_0 \exp(\int \alpha_{T,0} dT)$ at zero pressure and temperature T (see Refs. 24–31 listed below for the constants in these thermodynamic parameters); in addition, our γ_{isoth} distributions on isotherms at 2000 and 4000 K calculated using $w(V)T^2$ [and $w(V)T^3$] for the temperature-dependent part did not satisfy the three conditions discussed in Sec. III D as well as did the γ_{isoth} distributions for $w(V)T$.

²³J. Nguyen and N. Holmes, *Shock Compression in Condensed Matter-1999* (Elsevier, New York, 2000), p. 81.

²⁴L. Dubrovinsky, S. Saxena, F. Tutti, S. Rekhi, and T. LeBehan, Phys. Rev. Lett. **84**, 1720 (2000).

²⁵A. Jephcoat, H. Mao, and P. Bell, J. Geophys. Res. **91**, 4677 (1986).

²⁶E. Huang, W. Basset, and P. Tao, J. Geophys. Res. **92**, 8129 (1987).

²⁷N. Funamori, T. Yagi, and T. Uchida, Geophys. Res. Lett. **23**, 953 (1996).

²⁸S. Saxena, L. Dubrovinsky, P. Haggkvist, Y. Cerenius, G. Shen, and H.K. Mao, Science **269**, 1703 (1995).

²⁹L. Dubrovinsky, S. Saxena, and P. Lazor, Phys. Chem. Miner. **25**, 434 (1998).

³⁰L. Dubrovinsky, S. Saxena, and P. Lazor, Geophys. Res. Lett. **24**, 1835 (1997).

³¹L. Dubrovinsky, S. Saxena, and P. Lazor, Eur. J. Mineral. **10**, 43 (1998).